Arabidopsis thaliana telomeres exhibit euchromatic features

María I. Vaquero-Sedas, Francisco M. Gámez-Arjona and Miguel A. Vega-Palas*

Instituto de Bioquímica Vegetal y Fotosíntesis, Universidad de Sevilla – CSIC, c/ Américo Vespucio n° 49, 41092 Seville, Spain

ABSTRACT

Telomere function is influenced by chromatin structure and organization, which usually involves epigenetic modifications. We describe here the chromatin structure of *Arabidopsis thaliana* telomeres. Based on the study of six different epigenetic marks we show that *Arabidopsis* telomeres exhibit euchromatic features. In contrast, subtelomeric regions and telomeric sequences present at interstitial chromosomal loci are heterochromatic. Histone methyltransferases and the chromatin remodeling protein DDM1 control subtelomeric heterochromatin formation. Whereas histone methyltransferases are required for histone H3K9^{2Me} and non-CpG DNA methylation, DDM1 directs CpG methylation but not H3K9^{2Me} or non-CpG methylation. These results argue that both kinds of proteins participate in different pathways to reinforce subtelomeric heterochromatin formation.

INTRODUCTION

Telomeres play an essential role in cell biology because they contribute to maintain genome stability (1–3). Two basic models of telomeric chromatin organization have been described for telomeres that are replicated by telomerase. The first one can be found in *Saccharomyces cerevisiae*. In *Saccharomyces*, the telomeric repeat binding protein Rap1 binds to telomeres and nucleates the assembly of a nucleoprotein complex called telosome (4). Rap1 also recruits the Sir Silencing complex to subtelomeric regions leading to the formation of subtelomeric heterochromatin, which spreads ∼3 kb inside the chromosome (5,6). The integrity of this silencing complex is required for the proper function of telomeres (7,8). The second model of telomeric chromatin organization can be found in mouse where telomeres and subtelomeric regions are heterochromatic. The loss of heterochromatic marks causes telomere dysfunction in mouse, highlighting again the relevance of heterochromatin in telomeres biology (9).

Heterochromatin is highly condensed in interphase nuclei and exhibit defined molecular features including the methylation of DNA and of histone H3 lysine 9 (H3K9) (10–12). In *Arabidopsis*, heterochromatin is characterized by cytosine methylation, which can be targeted at CpG, CpNpG or CpNpN residues (where N is any nucleotide), and by H3K9^{1,2Me}, H3K27^{1,2Me} and H4K20^{1Me}. In turn, *Arabidopsis* euchromatin is characterized by H3K4^{1,2,3Me}, H3K36^{1,2,3Me}, H4K20^{2,3Me} and by histones acetylation (13). The levels of these epigenetic marks are regulated by a complex interplay of enzymatic and structural proteins. One of these proteins is the chromatin remodeling factor DDM1 (decrease in DNA methylation), a SWI2/SNF2 homolog. Mutations in *DDM1* cause loss of CpG methylation (14–16). CpG methylation have been found to control H3K9^{2Me} at different heterochromatic loci, which, in turn, direct non-CpG methylation (17–19). A high number of putative histone methyltransferases are present in *Arabidopsis* (10). Proteins that are known to be involved in the dimethylation of histone H3K9 include SUVH1, SUVH2, SUVH4, SUVH5 and SUVH6. Mutants lacking of SUVH4, also called KRYPTONYTE, have reduced levels of H3K9^{2Me} and non-CpG methylation at different heterochromatic loci (17,18). This decrease of epigenetic marks is more drastic in a triple mutant affected simultaneously in SUVH4, SUVH5 and SUVH6 (20).

Here, we describe the chromatin structure of *Arabidopsis thaliana* telomeres. We show that whereas telomeres exhibit euchromatic features, subtelomeric regions and interstitial telomeric sequences (ITSs) are heterochromatic. In addition, we show that histone methyltransferases and the chromatin remodeling protein DDM1 control subtelomeric heterochromatin formation. Finally, we compare our results with recently published data that also focus on the chromatin structure of *Arabidopsis* telomeres.

*To whom correspondence should be addressed. Tel: +34 954 489574; Fax: +34 954 460065; Email: vega-palas@ibvf.csic.es

MATERIALS AND METHODS

Plant material and growth conditions

Seeds from wild-type *Arabidopsis thaliana* (Columbia ecotype) and from mutant derivatives were obtained from the *Arabidopsis* Biological Resource Center (Ohio State University, Columbus, USA). The *ku70* mutant (SALK_123114) and the *suvh4* mutant (SALK_105816) were segregated to obtain homozygous lines that were verified by PCR. The Columbia (Col) *suvh4 suvh5 suvh6* mutant strain (*suvh4-6*) was a gift from Dr Judith Bender (Brown University, USA). This strain was made with a Col *suvh4* T-DNA insertion disruption into the 10th exon (SALK_044606) obtained from the *Arabidopsis* Biological Resource Center, the Col *suvh5-2* T-DNA insertion allele (20), and the Col *suvh6-1* T-DNA insertion allele (21). Each single *suvh* mutant was backcrossed two times to wild-type Col before being crossed together to make the triple *suvh4-6* mutant. The Columbia *ddm1* mutant strain used in this study was a gift from Dr Ingo Hoffmann (22). Plants were grown on soil at 22°C with a relative humidity of 70% during 3–4 weeks.

Methylation sensitivity analyses using restriction endonucleases

Southern blot analyses were performed using DNA isolated from rosette leaves following a CTAB based protocol (23). Essentially, 0.3–2 g of leaves were frozen on liquid nitrogen, ground and incubated at 65°C during 1 h in DNA extraction buffer (150 mM Tris pH 7.0; 1 M NaCl; 15 mM EDTA; 1.5% CTAB; 0.1% β-ME; 0.5% polyvinylpyrrolidine). Then, after chloroform extraction, DNA was precipitated with 0.6 volumes of isopropanol, RNase treated, phenolized and precipitated with ethanol. The purified DNA samples were digested with the corresponding restriction endonucleases, phenolized, precipitated with ethanol and resuspended in water. These DNA samples were resolved on agarose gels, transferred to Hybond™-XL membranes (GE Healthcare) and hybridized with a telomeric probe according to manufacturer instructions. Hybridizations were performed overnight at 65°C in the presence of 5× SSPE, 5× Denhardt's solution, 0.5% SDS and 40 µg/ml of denatured salmon sperm DNA. After hybridization, the membranes were washed three times at room temperature during 10 min with 2× SSPE plus 0.1% SDS and once at 65°C during 45 min with 1× SSPE and 0.1% SDS. The telomeric template used for hybridization was constructed by annealing and ligation of telomeric sequence oligos containing specific restriction sites at their ends. These sites were used for cloning in pUC18 (24). The sequence of the template is as follows: HindIII site – $(TTTAGGG)_{12}$ - SphI site – $(TTTAGGG)_{10}$ – SalI site - $(TTTAGGG)_{15}$ – EcoRI site. Prior to hybridization, it was excised from pUC18 using the HindIII and EcoRI sites, purified and labeled using a Ready-To-Go™ kit from GE Healthcare.

Chromatin immunoprecipitation

Wild-type or mutant leaves were used to perform ChIP assays as previously described (25). The antibody against 5-methylcytosine was provided by Merck, the antibodies against $H3K4^{2Me}$, $H3K9^{2Me}$ and $H3K27^{Me}$ were provided by Upstate Biotechnology and the antibodies against $H3K9^{Ac}$ and $H4K16^{Ac}$ were provided by Abcam. ChIP assays were analyzed by multiplex PCR or by hybridization. When the ChIP assays were analyzed by multiplex PCR, two sequential PCR reactions were performed. In the first one, the DNA was subjected to 22 cycles of amplification. In the second one, 1/100 of the first reaction was amplified. For each input and immunoprecipitated DNA sample, 4 second PCR reactions were performed at increasing number of cycles. Reactions in which the amount of PCR products increased exponentially were quantified and used for final figures. The oligos used for amplification are listed in Supplementary Table S1. Oligos used to display the euchromatic *CYP5* were included in all PCR reactions. To calculate enrichment values, the intensities of the PCR bands were quantified using the computer program Quantity One (BioRad). The intensity of the bands corresponding to the loci of interest were made relative to the intensity of the *CYP5* bands and normalized against the input samples. When the ChIP assays were analyzed by hybridization, the input and immunoprecipitated DNA samples were amplified following a whole genome amplification protocol to increase hybridization sensitivity (26). For each input and immunoprecipitated DNA sample, equal amounts of amplified DNA were either digested with Tru9I or undigested, resolved on agarose gels and hybridized with the telomeric probe as indicated in the previous section. Enrichment values were calculated as indicated in the legend of Figure 1.

RESULTS

Arabidopsis telomeres exhibit euchromatic features

Arabidopsis telomeres are composed of telomeric repeat arrays (of the TTTAGGG type) that are also abundant at interstitial chromosomal loci (27–32). Therefore, it is important to differentiate between telomeres and ITSs when telomeric studies are based on hybridizations with a telomeric probe. This problem has been previously addressed using frequently cutting restriction enzymes like Tru9I or MboI (33,34). Since *Arabidopsis* telomeres are composed of perfect telomeric repeat arrays, they remain uncut after digestion with the restriction enzymes. In contrast, ITSs are frequently cut because they are composed of very short arrays of perfect telomeric repeats interspersed with degenerated repeats (30,31,35,36). When *Arabidopsis* genomic DNA is digested with Tru9I and hybridized with a telomeric probe, most of the signals corresponding to ITSs disappear. Only three ITSs bands smaller than 500 bp remain (35). Therefore, the signals detected above 500 bp after Tru9I digestion correspond only to telomeres. In turn, the signals detected above 500 bp when the DNA is
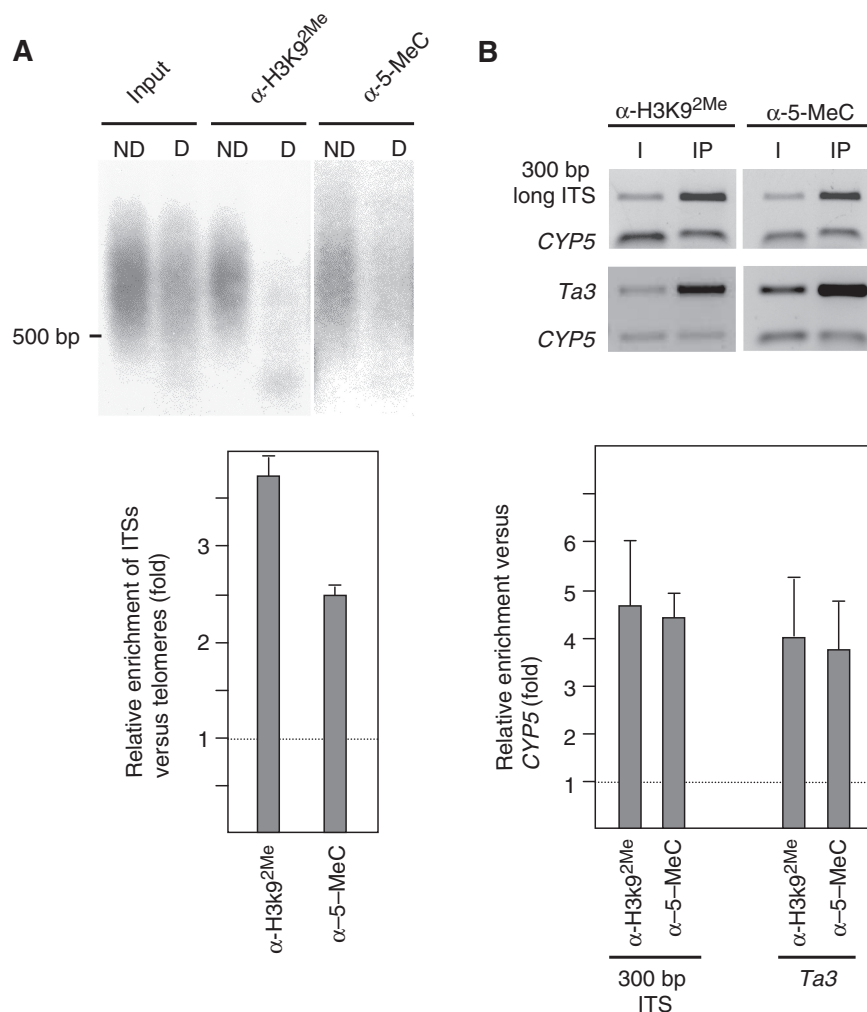
Figure 1. *Arabidopsis* telomeres exhibit euchromatic features. (**A**) Analysis of H3K9^{2Me} and 5-methylcytosine levels at telomeres and ITSs. ChIP experiments were performed using antibodies against H3K9^{2Me} (α-H3K9^{2Me}) and 5-methylcytosine (α-5-MeC). Input and immunoprecipitated DNA samples were amplified as indicated in the 'Materials and Methods' section. Then, equal amounts of DNA were digested with Tru9I or undigested, resolved on agarose gels and hybridized with the telomeric probe. D and ND indicate digested or not digested with Tru9I, respectively. Relative enrichment values of ITSs versus telomeres were calculated as follows: the intensity of the hybridization signals above 500 bp was quantified for all lanes. Whereas the signals of undigested samples corresponded to both, telomeres and ITSs, the signals of digested samples corresponded only to telomeres because telomeres are not digested by Tru9I. The relative amounts of ITSs versus telomeres present in the input and in the immunoprecipitated DNA samples were determined by comparing digested and undigested lanes. Relative enrichment values were calculated by dividing the relative amounts of ITSs versus telomeres in the immunoprecipitated DNA samples between the relative amounts found in the input samples. (**B**) Analysis of H3K9^{2Me} and 5-methylcytosine levels at a specific ITS and at the *Ta3* retrotransposon. The specific ITS studied was a 300-bp long telomeric repeats array present in the pericentromeric region of chromosome III (inside At3g33072). ChIP experiments were analyzed by multiplex PCR reactions including the *CYP5* gene as euchromatic reference. The *CYP5* gene corresponds always to the bottom band of the multiplex PCRs. I, input; IP, immunoprecipitated DNA. Graphic representations of enrichment values, calculated as indicated in the 'Materials and Methods' section, are shown at the bottom. Mean values of different experiments are represented together with the standard deviation.

undigested correspond to both, telomeres and ITSs (35). This observation has allowed us to study the chromatin structure of *Arabidopsis* telomeres and ITSs independently. After performing ChIP experiments, we amplified the input and the immunoprecipitated DNA samples following a whole genome amplification protocol, resolved the DNA samples undigested or digested with Tru9I in agarose gels and hybridized them with a telomeric probe (see 'Materials and Methods' section). Then, we calculated the relative enrichment of ITSs versus telomeres as indicated in the legend of Figure 1.

Since telomeres are composed of repetitive DNA sequences, which are usually organized as heterochromatin, we decided to study whether *Arabidopsis* telomeres exhibit heterochromatic features. As mentioned above, H3K9^{2Me} and cytosine methylation are diagnostic hallmarks that label *Arabidopsis* heterochromatin (18,19). We analyzed these heterochromatic modifications at *Arabidopsis* telomeres and ITSs and found that ITSs had higher levels than telomeres (Figure 1A). After immunoprecipitation with the antibody against H3K9^{2Me}, ITSs were enriched 3.7 times versus telomeres. Similarly, ITSs were enriched 2.5 times after 5-methylcytosine immunoprecipitation.

To further characterize the enhanced levels of heterochromatic marks present at ITSs, we studied a specific 300-bp long ITS present in the pericentromeric region of

Arabidopsis chromosome III. We analyzed the levels of $H3K9^{2Me}$ and 5-methylcytosine at this locus by multiplex PCR including the euchromatic *CYP5* gene as a reference. As expected, the 300-bp long ITS showed higher levels of $H3K9^{2Me}$ and 5-methylcytosine than *CYP5*, 4.7 and 4.5 times higher, respectively (Figure 1B). Similar levels of heterochromatic marks were found at the *Ta3* retrotransposon (Figure 1B), which has been previously shown to be heterochromatic. Since these levels of enrichment were similar to the levels of ITSs enrichment versus telomeres, we concluded that, whereas ITSs are heterochromatic, telomeres exhibit euchromatic features.

The results mentioned above were very surprising because telomeres have been traditionally considered as part of the heterochromatin present in the cell nucleus. Therefore, we decided to corroborate the euchromatic nature of *Arabidopsis* telomeres by studying four additional histone modifications: histone $H3K4^{2Me}$, histone $H3K27^{Me}$ and histones H3K9 and H4K16 acetylation ($H3K9^{Ac}$, $H4K16^{Ac}$). It is known that *Arabidopsis* heterochromatin have lower levels of $H3K4^{2Me}$, $H3K9^{Ac}$ and $H4K16^{Ac}$ than euchromatin. In contrast, heterochromatin in *Arabidopsis* has higher levels of $H3K27^{Me}$ (13). We determined the levels of ITSs enrichment versus telomeres for all these epigenetic modifications. The results obtained for each chromatin marker were consistent with a euchromatic structure for telomeres and an heterochromatic structure for ITSs (Figure 2).

As mentioned above, we amplified the input and the immunoprecipitated DNA samples before hybridization. During this process we noticed that telomeres were amplified more efficiently than ITSs. Before amplification, telomeres generated ~30–40% of the signal displayed when the input samples were hybridized with the telomeric probe. After amplification, telomeres generated 80% of the input signal. We assumed that this amplification bias did not affect the calculation of relative enrichment values because they were calculated by comparing input and immunoprecipitated DNA samples. To support this notion, we analyzed unamplified input and immunoprecipitated DNA samples obtained with α-$H3K27^{Me}$ and α-$H3K9^{2Me}$ (Supplementary Figure S1). We estimated the relative amounts of *CYP5* in these samples and calculated the relative enrichment of ITSs versus telomeres and of telomeres versus *CYP5*. We found that ITSs had higher levels of $H3K27^{Me}$ and α-$H3K9^{2Me}$ than telomeres, which were similar to the levels determined with the amplified DNA samples (Figures 1 and 2). In addition, we found that telomeres had levels of $H3K27^{Me}$ and α-$H3K9^{2Me}$ similar to the euchromatic *CYP5* gene (Supplementary Figure S1). These results further supported the euchromatic nature of *Arabidopsis* telomeres.

Subtelomeric regions organize as well defined heterochromatin domains

Since subtelomeric regions usually organize as heterochromatin, we decided to analyze the levels of DNA methylation and histone $H3K9^{2Me}$ in the subtelomeric regions of *Arabidopsis*. We studied $H3K9^{2Me}$ at different
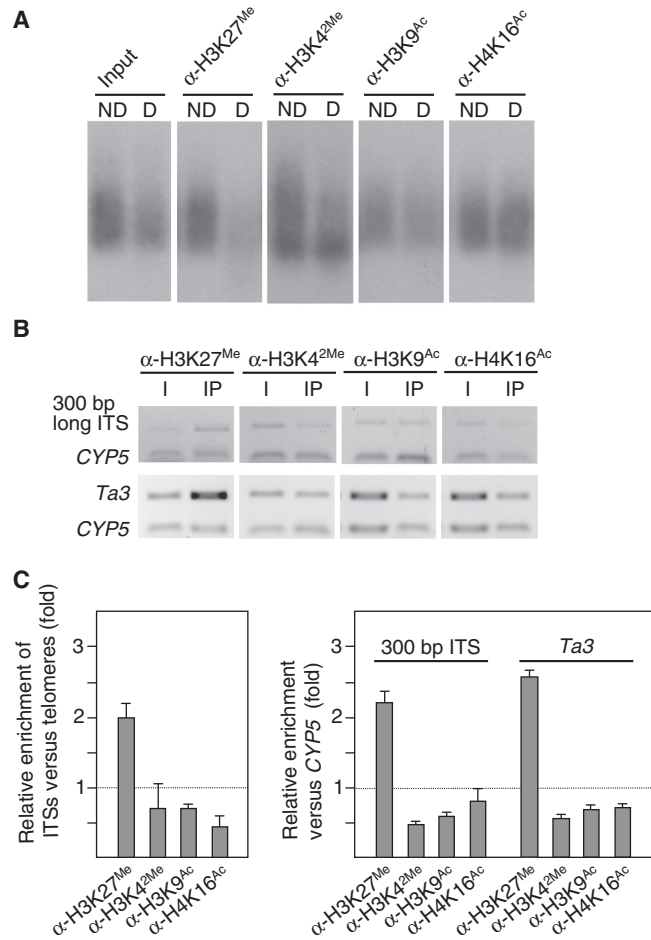

Figure 2. Additional euchromatic features present at *Arabidopsis* telomeres. (**A**) Analysis of $H3K27^{Me}$, $H3K4^{2Me}$, $H3K9^{Ac}$ and $H4K16^{Ac}$ levels at telomeres and ITSs. ChIP experiments were performed using antibodies against $H3K27^{Me}$ (α-$H3K27^{Me}$), $H3K4^{2Me}$ (α-$H3K4^{2Me}$), $H3K9^{Ac}$ (α-$H3K9^{Ac}$) and $H4K16^{Ac}$ (α-$H4K16^{Ac}$). Input and immunoprecipitated DNA samples were amplified as indicated in the 'Materials and Methods' section. Then, equal amounts of DNA were digested with Tru9I (D) or undigested (ND), resolved on agarose gels and hybridized with the telomeric probe. (**B**) Analysis of $H3K27^{Me}$, $H3K4^{2Me}$, $H3K9^{Ac}$ and $H4K16^{Ac}$ levels at the 300-bp long ITS and at the *Ta3* retrotransposon. ChIP experiments were analyzed by multiplex PCR reactions including the *CYP5* gene as euchromatic reference. The *CYP5* gene corresponds always to the bottom band of the multiplex PCR. I, input; IP, immunoprecipitated DNA. (**C**) Graphic representation of relative enrichment values of ITSs versus telomeres, of *Ta3* versus *CYP5* and of the 300-bp long ITS versus *CYP5*.

subtelomeric positions in the left arm of chromosome I and in the right arm of chromosome IV (IL and IVR, respectively). $H3K9^{2Me}$ enrichment was observed from the telomeric repeats borders up to ~1 kb in IL and up to around to 2 kb in IVR (Figure 3A and B). However, it was not detected further inside the chromosomes, indicating that these $H3K9^{2Me}$ domains are small and well defined. We performed *in silico* analyses of the subtelomeric regions present in IL and in IVR looking for repetitive DNA sequences and found that whereas the subtelomeric region present in IVR is mostly repetitive up to 2 kb, subtelomeric sequences in IL are essentially non-

repetitive (see black rectangles in Figure 3). Therefore, extensive repetitiveness at subtelomeric regions is not required for H3K9^{2Me} enrichment although it might influence H3K9^{2Me} levels.

We mapped subtelomeric DNA methylation using an experimental approach that allowed us to analyze the average methylation state of all the subtelomeric regions and of ITSs simultaneously. First, we used two restriction endonucleases, BstNI and EcoRII, which are two isoschizomers that cut a 5-bp DNA sequence motif (CCWGG). Whereas BstNI is insensitive to DNA methylation and digests all their DNA targets, EcoRII is sensitive to CpNpG or CpNpN methylation and does not digest targets that contain methylated cytosines. Therefore, BstNI and EcoRII allow detection of non-CpG methylation. We digested wild-type *Arabidopsis* DNA samples with these restriction enzymes, resolved them on agarose gels and displayed telomeres and ITSs digestion profiles by hybridization with the telomeric probe. To distinguish telomeres from ITSs, we also analyzed DNA from a *ku70* mutant, which has longer telomeres than the wild-type (37). Telomeric bands from *ku70* migrate slower in the gel than wild-type telomeric

bands. In contrast, wild-type and *ku70* bands corresponding to ITSs migrate at the same distance. A smeared band of ~2.5–5 kb was detected after digesting wild-type genomic DNA with BstNI (indicated by a rectangle in Figure 4A). This band corresponded to telomeres because it shifted upwards in the gel in the *ku70* mutant (Figure 4A). This telomeric band was ~1–2 kb shorter than the telomeric band observed after digesting wild-type DNA with EcoRII (Figure 4A). Therefore, we concluded that subtelomeric regions undergo non-CpG methylation up to ~1–2 kb from the telomeric repeats border. The lower molecular weight bands observed after digesting wild-type DNA with BstNI corresponded to ITSs because they were also present in the *ku70* mutant. These bands were not detected when wild-type and *ku70* genomic DNA samples were digested with EcoRII. Instead, higher molecular weight smears were detected at the top of the EcoRII lanes indicating that ITSs undergo non-CpG methylation.

We also mapped subtelomeric DNA methylation using MspI and HpaII (Figure 4B). These enzymes are two isoschizomers that cut a 4-bp DNA sequence motif
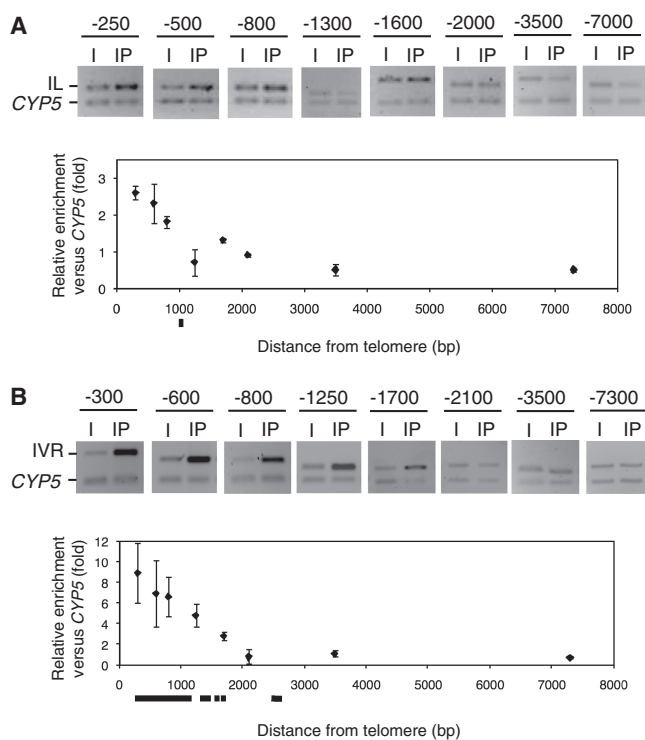

Figure 3. Subtelomeric regions undergo H3K9^{2Me}. (**A**) H3K9^{2Me} levels at the left telomeric region of chromosome I (IL). ChIP experiments were analyzed by multiplex PCR using the *CYP5* gene as euchromatic reference. The *CYP5* gene corresponds always to the bottom band of the multiplex PCRs. I, input; IP, immunoprecipitated DNA. H3K9^{2Me} levels were analyzed at different distances from the centromeric border of telomere IL. These distances (in bp) are indicated at the top of each panel. Relative enrichment values are represented at the bottom. Subtelomeric DNA regions longer than 50 bp that share >80% of identity with at least one different region of the genome are indicated by black rectangles. (**B**) H3K9^{2Me} levels at the right telomeric region of chromosome IV (IVR).
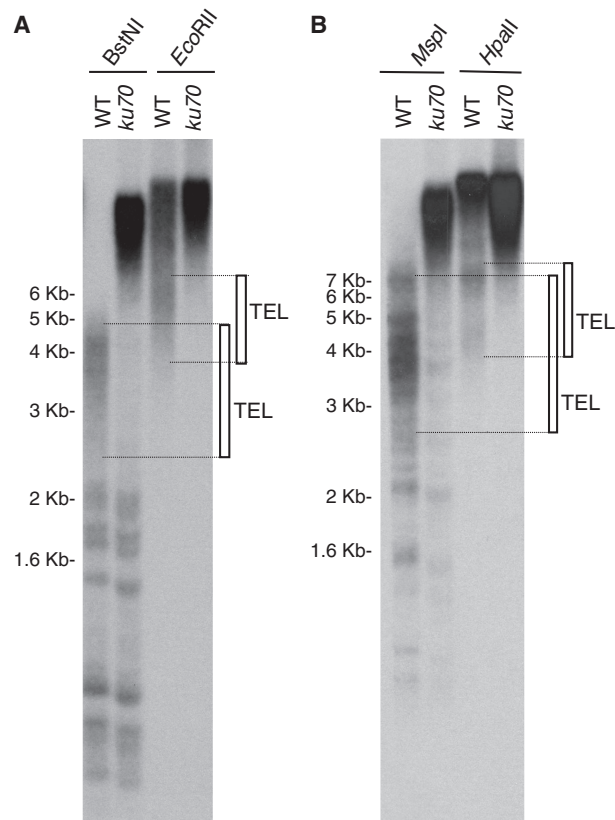

Figure 4. Subtelomeric regions undergo DNA methylation. (**A**) Southern blot analysis of *Arabidopsis* genomic DNA digested with BstNI or EcoRII and hybridized with the telomeric probe. Wild-type (WT) and *ku70* genomic DNA samples were digested with the restriction enzymes, resolved on an agarose gel and hybridized. The migration distances of molecular weight markers are indicated on the left. Rectangles on the right indicate the position of wild-type telomeric bands (TEL). (**B**) Southern blot analysis of *Arabidopsis* genomic DNA digested with MspI or HpaII and hybridized with the telomeric probe.

(CCGG). Whereas MspI is sensitive to CpNpG methylation, HpaII is sensitive to CpG and CpNpG methylation. Therefore, the comparison of the digestion profiles generated by these enzymes indicates the presence or absence of CpG methylation. The fuzzy telomeric band generated after digesting wild-type genomic DNA with MspI was 1–2 kb shorter than the telomeric band generated after digesting wild-type DNA with HpaII (Figure 4B). Therefore, we concluded that subtelomeric regions undergo CpG methylation. The extent of this DNA methylation is in close agreement with the extent of DNA methylation detected with BstNI and EcoRII and with the extent of $H3K9^{2Me}$ enrichment detected in IL and IVR. These results indicated that subtelomeric regions in *Arabidopsis* organize as small and well-defined heterochromatin domains characterized by DNA and histone H3K9 methylation.

To further characterize subtelomeric heterochromatin, we analyzed the levels of three euchromatic marks in IL and in IVR (Figure 5). These marks were $H3K4^{2Me}$, $H3K9^{Ac}$ and $H4K16^{Ac}$. We found that both subtelomeric regions had lower levels of all these marks than *CYP5*. These levels were similar to those present in the *Ta3* retrotransposon (Figure 5). Therefore, subtelomeric regions seem to have the typical heterochromatin structure found at other genomic loci in *Arabidopsis*. These results are supported by high-resolution genomic maps (http://epigenomics.mcdb.ucla.edu) (38–40).

Histone methyltransferases control subtelomeric DNA and histone H3K9 methylation

To start deciphering the molecular basis responsible for the formation of subtelomeric heterochromatin, we decided to study histone methyltransferase mutants. Histone methyltransferases are conserved in eukaryotes and control heterochromatin formation (41). There are many putative histone methyltransferase genes in *Arabidopsis* (10). Some of these genes are involved in $H3K9^{2Me}$. A triple mutant affected in three histone methyltransferases (*suvh4, suvh5 and suvh6*; herein referred to as *suvh4-6*) has been previously found to lose $H3K9^{2Me}$ and non-CpG methylation at different target loci (20). We analyzed the levels of histone $H3K9^{2Me}$ at subtelomeric regions in this triple mutant. We found that *suvh4-6* had levels of subtelomeric $H3K9^{2Me}$ similar to those present in *CYP5* (Figure 6). Therefore, we concluded that subtelomeric heterochromatin formation was altered in this mutant. Interestingly, subtelomeric $H3K9^{2Me}$ was decreased but not completely lost in a single *suvh4* mutant (also named *kyp*), indicating that the establishment of subtelomeric $H3K9^{2Me}$ involves multiple histone methyltransferases (Supplementary Figure S2).

To analyze whether the triple *suvh4-6* mutant was affected in subtelomeric DNA methylation, we studied the levels of 5-methylcytosine at different subtelomeric positions by ChIP (Figure 6). As previously shown for $H3K9^{2Me}$, we found that cytosine methylation was enriched in IVR up to ~2 kb in the wild-type strain. However, although cytosine methylation could also be
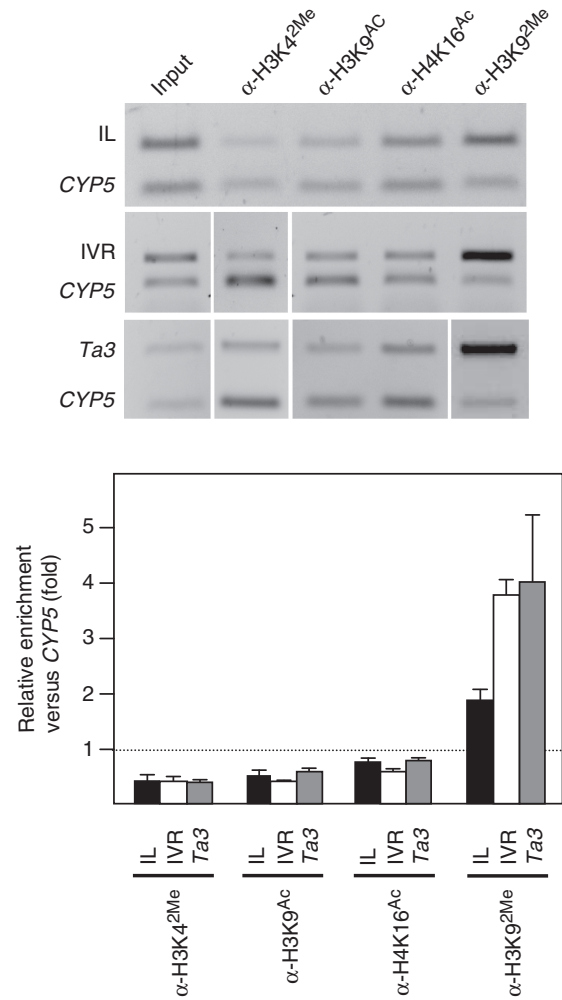

Figure 5. Subtelomeric regions have similar levels of euchromatic marks than *Ta3*. Different euchromatic marks ($H3K4^{2Me}$, $H3K9^{Ac}$ and $H4K16^{Ac}$) were analyzed at 500 bp from the centromeric border of telomere IL, at 600 bp from the centromeric border of telomere IVR and at the *Ta3* retrotransposon. A heterochromatic mark ($H3K9^{2Me}$) was included as a control. ChIP experiments were analyzed by multiplex PCR using the *CYP5* gene as euchromatic reference. The *CYP5* gene corresponds always to the bottom band of the multiplex PCRs. Relative enrichment values are represented at the bottom together with the standard deviation.

observed in the *suvh4-6* mutant, the levels of methylation enrichment were lower in the mutant than in the wild-type. To study whether the lower levels of cytosine methylation found in the mutant involved the loss of non-CpG methylation, we performed methylation sensitivity analyses using HpaII, MspI, BstNI and EcoRII (Figure 7). We digested suvh4-6 DNA with these restriction enzymes and hybridized the resulting DNA samples with the telomeric probe. As a control, we also analyzed wild-type DNA. The fuzzy telomeric band generated after digesting *suvh4-6* DNA with HpaII was longer than the telomeric band generated after digesting the same DNA with MspI (see white lines in Figure 7A). Since similar differences were observed with wild-type DNA, we concluded that subtelomeric CpG methylation largely remained in the mutant. Therefore, the lower levels of cytosine
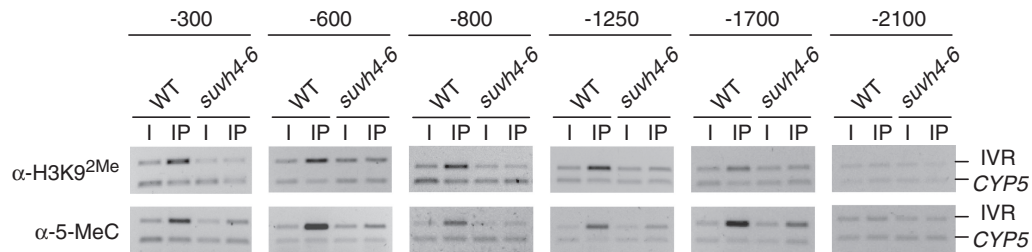
Figure 6. Histone methyltransferases control subtelomeric H3K9^{2Me} and DNA methylation. H3K9^{2Me} and DNA methylation levels were analyzed at the right telomeric region of chromosome IV. WT refers to wild-type *Arabidopsis* whereas *suvh4-6* refers to a triple mutant affected simultaneously in *SUVH4, SUVH5* and *SUVH6*. ChIP experiments were analyzed by multiplex PCR using the *CYP5* gene as euchromatic reference. The *CYP5* gene corresponds always to the bottom band of the multiplex PCRs. I, input; IP, immunoprecipitated DNA. Distances from the centromeric border of telomere IVR (in bp) are indicated at the top of the figure.
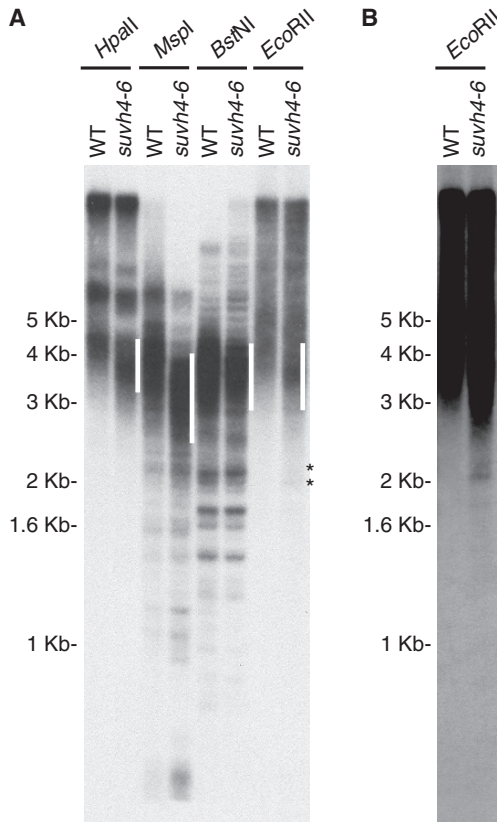

Figure 7. Histone methyltransferases control subtelomeric non-CpG methylation. (**A**) Southern blot analysis of wild-type (WT) and *suvh4-6* genomic DNA digested with HpaII, MspI, BstNI or EcoRII and hybridized with the telomeric probe. The migration distances of molecular weight markers are indicated on the left. White lines indicate the position of the main *suvh4-6* telomeric bands. Asterisks indicate ITSs bands generated after digesting *suvh4-6* DNA with EcoRII. (**B**) Longer exposure of the lanes containing wild-type and *suvh4-6* DNA digested with EcoRII. Asterisks indicate ITSs bands.

methylation detected by ChIP in *suvh4-6* should be due to the loss of non-CpG methylation. The restriction profiles obtained with BstNI and EcoRII confirmed this conclusion because the *suvh4-6* telomeric bands generated by these enzymes had similar average size (see white lines in Figure 7A). In addition, the restriction profiles generated after digesting wild-type and *suvh4-6* DNA with MspI and EcoRII indicated that ITSs methylation was also affected

in the mutant (Figure 7A and B). ITSs were digested more extensively by these enzymes in the *suvh4-6* mutant than in the wild-type (see low molecular weight bands including those marked with asterisks). These results indicated that part of the non-CpG methylation associated with ITSs was affected in the mutant.

DDM1 controls subtelomeric DNA methylation

To further characterize subtelomeric heterochromatin we decided to study a *ddm1* mutant. DDM1 is a chromatin remodeling protein that is required for heterochromatin formation in *Arabidopsis*. The *ddm1* mutant loses CpG methylation and have reduced non-CpG methylation at different heterochromatic loci (14–16). We analyzed subtelomeric DNA methylation in this mutant by using HpaII, MspI, BstNI and EcoRII (Figure 8). As previously shown, the fuzzy telomeric band generated by MspI after digesting wild-type DNA and hybridizing it with the telomeric probe was shorter than the telomeric band generated after digesting the same DNA with HpaII. However, the telomeric bands generated after digesting *ddm1* DNA with both enzymes had similar size. These results indicated that subtelomeric CpG methylation was lost in the *ddm1* mutant. By contrast, the restriction profiles generated by BstNI and EcoRII revealed that subtelomeric non-CpG methylation largely remained in the mutant because the telomeric band generated by EcoRII after digesting *suvh4-6* DNA was longer than the telomeric band generated by BstNI after digesting the same DNA. In addition, the restriction profiles generated with MspI and HpaII revealed that CpG methylation was also lost at ITSs in the *ddm1* mutant (Figure 8). The low molecular weight ITSs bands generated after digesting wild-type DNA with MspI were not detected after HpaII digestion. However, these bands were readily detected after digesting *ddm1* DNA with MspI or with HpaII.

We analyzed subtelomeric H3K9^{2Me} and 5-methylcytosine by ChIP in the *ddm1* mutant. As a control, we also analyzed the *Ta3* retrotransposon (Figure 9). We found that the levels of H3K9^{2Me} and 5-methylcytosine were reduced at the *Ta3* retrotransposon in the mutant. However, the levels of these epigenetic marks were not reduced at subtelomeric regions. These results argue that most of the subtelomeric DNA
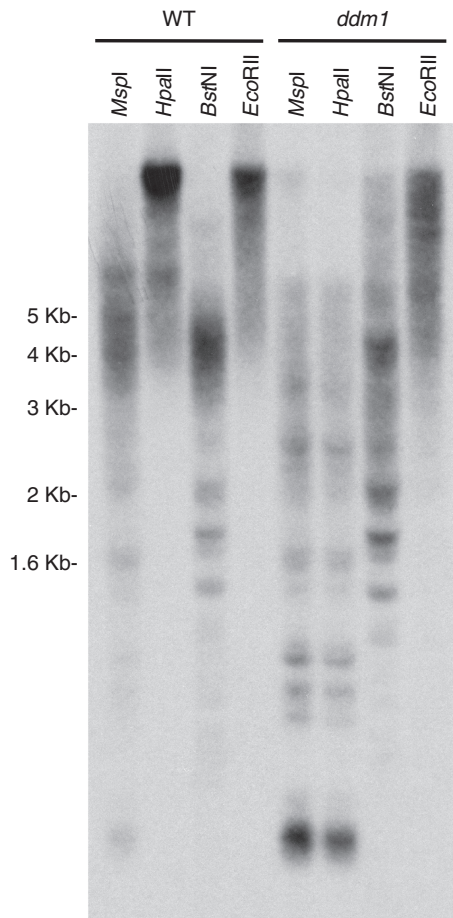
Figure 8. DDM1 controls subtelomeric DNA methylation. A Southern blot analysis of wild-type (WT) and *ddm1* genomic DNA digested with HpaII, MspI, BstNI or EcoRII and hybridized with the telomeric probe is shown. The migration distances of molecular weight markers are indicated on the left.

Figure 9. CpG methylation is not required for H3K9^{2Me} at subtelomeric heterochromatin. H3K9^{2Me} and DNA methylation levels were analyzed at the right telomeric region of chromosome IV. WT refers to wild-type *Arabidopsis*. ChIP experiments were analyzed by multiplex PCR using the *CYP5* gene as euchromatic reference. The *CYP5* gene corresponds always to the bottom band of the multiplex PCRs. I, input; IP, immunoprecipitated DNA. Distances from the centromeric border of telomere IVR are indicated in the left. Relative enrichment values are represented at the bottom together with the standard deviation.

methylation is of the non-CpG type and indicate that neither DDM1 nor CpG methylation are required for H3K9^{2Me} or for non-CpG methylation at subtelomeric regions.

DISCUSSION

Arabidopsis telomeres represent a novel type of telomeric chromatin organization

Two basic types of telomeric chromatin organization have been previously described for telomeres that are replicated by telomerase. The first one can be found in *Saccharomyces cerevisiae* and consist of short telomeres that associate with a multiprotein complex and subtelomeric regions that are heterochromatic (4,5). The second model can be found in mouse where telomeres and subtelomeric regions associate with heterochromatic marks (9). We have found that *Arabidopsis* telomeres exhibit euchromatic features whereas subtelomeric regions are heterochromatic. Therefore, *Arabidopsis* represents a novel type of telomeric chromatin organization.
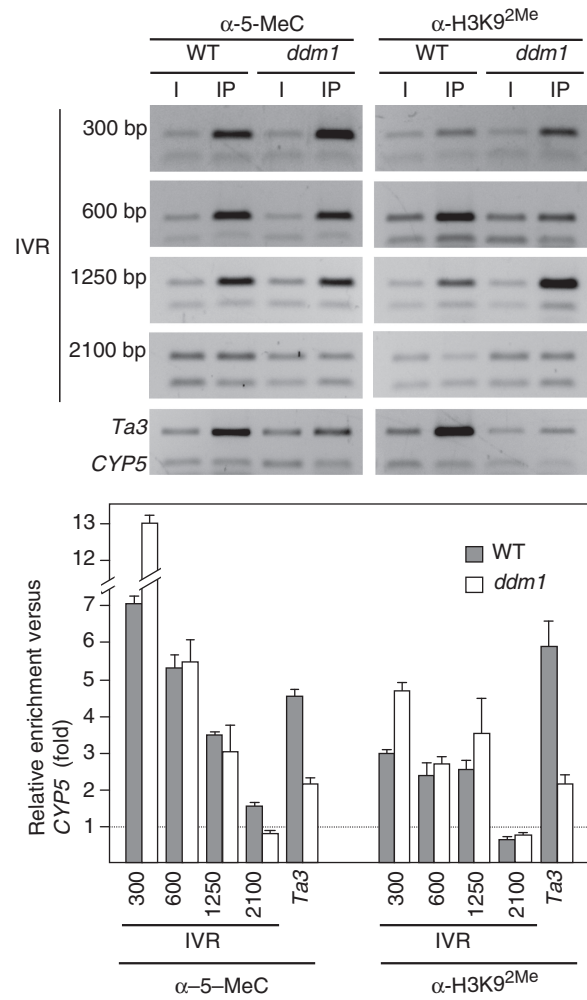
Arabidopsis heterochromatin share more similarities with mouse than with *Saccharomyces* heterochromatin. Actually, *Saccharomyces* heterochromatin is rather different from the heterochromatin found in most eukaryotes. It is characterized by low levels of histones acetylation and by the absence of DNA methylation (42). In turn, although heterochromatin in many eukaryotes is also characterized by histones hypoacetylation, it usually contains methylation marks that are not present in *Saccharomyces* heterochromatin (13,42). Mouse telomeric and/or subtelomeric heterochromatin have been found to contain low levels of histones H3 and H4 acetylation and high levels of histone H3K9^{3Me}, histone H4K20^{3Me} and DNA methylation (9). Similarly, we have found that *Arabidopsis* subtelomeric heterochromatin has low levels of histones H3K9 and H4K16 acetylation, low levels of

histone H3K4^{2Me} and high levels of histone H3K9^{2Me} and DNA methylation. Our results are in agreement with data published in a recent report by Vrbsky and colleagues (43). In this report, they described high levels of subtelomeric histone H3K9^{2Me}, histone H3K27^{Me} and DNA methylation in *Arabidopsis*.

We have found that histone methyltransferases and the chromatin remodeling protein DDM1 control subtelomeric heterochromatin formation in *Arabidopsis*. These proteins contribute to label subtelomeric heterochromatin with different epigenetic marks. Whereas histone methyltransferases are required for H3K9^{2Me} and non-CpG methylation, DDM1 is required for CpG methylation. Neither DDM1 nor CpG methylation are needed for H3K9^{2Me} or for non-CpG methylation at subtelomeric regions. However, DDM1 and CpG methylation influence H3K9^{2Me} and non-CpG methylation at other heterochromatic loci, including the *Ta3* retrotransposon (Figure 9) (14–19). These results reflect that some of the molecular mechanisms involved in the formation of subtelomeric heterochromatin might differ from those found at other heterochromatic loci. In addition, these results argue that both kinds of proteins, histone methyltransferases and DDM1, participate in different pathways to reinforce subtelomeric heterochromatin formation. Vrbsky and colleagues have shown that the RNA dependent DNA Methylation pathway (RdDM) is involved in the formation of subtelomeric heterochromatin in *Arabidopsis* (43). An *rdr2* mutant, which is affected in this pathway, was shown to have lower levels of DNA methylation and histone H3K9^{2Me} than the wild-type at subtelomeric regions (43). Here, we have identified the SUVH4-6 proteins as members of this pathway. In a complementary way, DDM1 could participate in the maintenance of subtelomeric CpG methylation associated with the replication of the DNA (44,45).

Vrbsky and colleagues analyzed the chromatin structure of *Arabidopsis* telomeres and proposed that they exhibit features of intermediate heterochromatin that extend to subtelomeric regions (43). This intermediate heterochromatin was proposed to contain both repressive and active epigenetic marks. The repressive marks were DNA methylation, H3K27^{Me} and H3K9^{2Me}. The active mark was H3K4^{3Me}. Here, we report that *Arabidopsis* telomeres exhibit euchromatic features whereas subtelomeric regions are heterochromatic. Our conclusions are based on the analysis of six different epigenetic marks including DNA methylation, H3K27^{Me} and H3K9^{2Me}. We understand that the discrepancies between the data published by Vrbsky and colleagues and our results rely on the different methodological approaches that we have followed to analyze epigenetic marks.

To analyze histone H3 epigenetic modifications at telomeres, Vrbsky and colleagues performed ChIP experiments with different antibodies, dot-blotted the input and the immunoprecipitated DNA samples and hybridized them with a telomeric probe. They also hybridized bysulfite treated DNA with the telomeric probe to analyze DNA methylation at telomeres. Although they were aware of the presence of ITSs in the *Arabidopsis* genome, they assumed that only telomeres were detected in those studies. This assumption relied on some experimental data that they showed (43). They digested *Arabidopsis* genomic DNA with TruI1, resolved the resulting DNA fragments in a gel and hybridized them at high stringency (65°C) with the telomeric probe. After hybridization, they found that most of the signal corresponded to telomeres. Therefore, they concluded that only telomeres were detected in the chromatin structure analyses. We have published essentially the same experiment mentioned above but using Tru9I, an isoschizomer of TruI1 (35). We also found that most of the hybridization signal corresponded to telomeres after Tru9I digestion. However, if the genomic DNA was not digested with Tru9I before hybridization, we found that most of the signal corresponded to ITSs (35). As mentioned above, ITSs are barely detected after *Tru*9I digestion because most of them are sliced to a size that do not hybridize with the telomeric probe. In contrast, telomeres are readily detected after Tru9I digestion because they are essentially composed of perfect telomeric repeats, which are not cut by the enzyme (35). Since Vrbsky and colleagues analyzed the chromatin structure of *Arabidopsis* telomeres by hybridizing DNA samples undigested with TruI1, we believe that they did not analyze the chromatin structure of true telomeres. We think that they analyzed a mix of euchromatic telomeres and heterochromatic ITSs.

Vrbsky and colleagues proposed that subtelomeric regions have an intermediate heterochromatin structure because they found subtelomeric enrichment of a euchromatic mark (H3K4^{3Me}). This result does not agree with high-resolution genomic maps (http://epigenomics.mcdb.ucla.edu) (40). Therefore, we believe that the levels of H3K4^{3Me} at subtelomeric regions should be further analyzed by quantitative methods.

Arabidopsis telomeres might impair heterochromatin formation

We have shown that subtelomeric heterochromatin occupy small and well-defined domains in *Arabidopsis*. This heterochromatin might be recruited by telomeric proteins and, then, spread inside the chromosome following a sequential mechanism. However, subtelomeric heterochromatin does not spread through telomeres towards the chromosome end, which might reflect that *Arabidopsis* telomeres impair heterochromatin formation.

In *Arabidopsis*, like in other eukaryotes, the RNAi pathway participates in the heterochromatinization of repetitive sequences. This pathway involves the action of siRNAs which, in principle, should be able to target any nuclear compartment (45,46). There are siRNAs containing telomeric sequences in *Arabidopsis* (http://asrp.cgrb.oregonstate.edu) (43,47). These telomeric siRNAs, together with other components of the RNAi pathway, should be involved in the heterochromatinization of *Arabidopsis* ITSs. However, telomeric siRNAs do not induce telomeres heterochromatinization. We believe that some molecular or architectural features of *Arabidopsis* telomeres might impair siRNAs induced heterochromatin formation. Some boundary elements might localize at the telomeric/subtelomeric transition

regions and contribute to maintain the euchromatic state of telomeres and/or to prevent subtelomeric heterochromatin from spreading into telomeres. The subtelomeric regions that abut *Arabidopsis* telomeres usually contain degenerated telomeric repeats, which could be bound by many of the putative telomeric repeat binding factors present in the plant (48). It will be interesting to investigate the influence of these degenerated repeats and of the D-Loop formation on the chromatin organization of *Arabidopsis* telomeric and subtelomeric regions.

The heterochromatic nature of *Arabidopsis* ITSs might contribute to confer genomic stability

As mentioned above, whereas telomeres localize at the end of eukaryotic chromosomes and are essentially composed of perfect telomeric repeats, *Arabidopsis* ITSs are mainly pericentromeric and contain few perfect telomeric repeats interspersed with degenerated repeats (27–32,35,36). We have shown that *Arabidopsis* ITSs are heterochromatic, which might be influenced by their pericentromeric localization. However, how the differential environment and the primary sequence of *Arabidopsis* telomeres and ITSs influence their chromatin organization should be the subject of future studies. In general, ITSs have been related to chromosomal aberrations, fragile sites, hot spots for recombination and diseases caused by genomic instability (49). In *Arabidopsis,* the lack of telomerase and of the XPF-ERCC1 endonuclease leads to developmental problems that are accompanied by genomic instability. This instability involves high levels of recombination events between telomeric regions and ITSs (36), which in the wild-type strain probably occur with low frequency. Since heterochromatin is known to inhibit repeated DNA recombination (50), we believe that the heterochromatic nature of *Arabidopsis* ITSs might contribute to prevent genomic instability.

SUPPLEMENTARY DATA

Supplementary Data are available at NAR Online.

REFERENCES

1. Cech,T. (2004) Beginning to understand the end of the chromosome. *Cell*, **43**, 405–413.
2. Blackburn,E. (2005) Telomeres and telomerase: their mechanisms of action and the effects of altering their functions. *FEBS Lett.*, **579**, 859–862.
3. Greider,C. (2006) Telomerase RNA levels limit the telomere length equilibrium. *Cold Spring Harb. Symp. Quant. Biol.*, **71**, 225–229.
4. Wright,J., Gottschling,D. and Zakian,V. (1992) *Saccharomyces* telomeres assume a non-nucleosomal chromatin structure. *Genes Dev.*, **6**, 197–210.
5. Hecht,A., Strahl-Bolsinger,S. and Grunstein,M. (1996) Spreading of transcriptional repressor SIR3 from telomeric heterochromatin. *Nature*, **383**, 92–96.
6. Luo,K., Vega-Palas,M. and Grunstein,M. (2002) Rap1-Sir4 binding independent of other Sir, yKu, or histone interactions initiates the assembly of telomeric heterochromatin in yeast. *Genes Dev.*, **16**, 1528–1539.
7. Lustig,A., Kurtz,S. and Shore,D. (1990) Involvement of the silencer and UAS binding protein RAP1 in regulation of telomere length. *Science*, **250**, 549–553.
8. Palladino,F., Laroche,T., Gilson,E., Axelrod,A., Pillus,L. and Gasser,S. (1993) SIR3 and SIR4 proteins are required for the positioning and integrity of yeast telomeres. *Cell*, **75**, 543–555.
9. Blasco,M. (2007) The epigenetic regulation of mammalian telomeres. *Nat. Rev. Genet.*, **8**, 299–309.
10. Fischer,A., Hofmann,I., Naumann,K. and Reuter,G. (2006) Heterochromatin proteins and the control of heterochromatic gene silencing in *Arabidopsis*. *J. Plant Phys.*, **163**, 358–368.
11. Jenuwein,T. (2006) The epigenetic magic of histone lysine methylation. *FEBS J.*, **273**, 3121–3135.
12. Grewal,S. and Jia,S. (2007) Heterochromatin revisited. *Nat. Rev. Genet.*, **8**, 35–46.
13. Fuchs,J., Demidov,D., Houben,A. and Schubert,I. (2006) Chromosomal histone modification patterns-from conservation to diversity. *Trends Plant Sci.*, **11**, 199–208.
14. Vongs,A., Kakutani,T., Martienssen,R. and Richards,E. (1993) *Arabidopsis thaliana* DNA methylation mutants. *Science*, **260**, 1926–1928.
15. Ronemus,M., Galbiati,M., Ticknor,C., Chen,J. and Dellaporta,S. (1996) Demethylation-induced developmental pleiotropy in *Arabidopsis*. *Science*, **273**, 654–657.
16. Jeddeloh,J., Stokes,T. and Richards,E. (1999) Maintenance of genomic methylation requires a SWI2/SNF2-like protein. *Nat. Genet.*, **22**, 94–97.
17. Jackson,J., Lindroth,A., Cao,X. and Jacobsen,S. (2002) Control of CpNpG DNA methylation by the KRYPTONITE histone H3 methyltransferase. *Nature*, **416**, 556–560.
18. Johnson,L., Cao,X. and Jacobsen,S. (2002) Interplay between two epigenetic marks: DNA methylation and histone H3 lysine 9 methylation. *Curr. Biol.*, **12**, 1360–1367.
19. Soppe,W., Jasencakova,Z., Houben,A., Kakutani,T., Meister,A., Huang,M., Jacobsen,S., Schubert,I. and Fransz,P. (2002) DNA methylation controls histone H3 lysine 9 methylation and heterochromatin assembly in *Arabidopsis*. *EMBO J.*, **21**, 6549–6559.
20. Ebbs,M. and Bender,J. (2006) Locus-specific control of DNA methylation by the *Arabidopsis* SUVH5 histone methyltransferase. *Plant Cell*, **18**, 1166–1176.
21. Ebbs,M., Bartee,L. and Bender,J. (2005) H3 lysine 9 methylation is maintained on a transcribed inverted repeat by combined action of SUVH6 and SUVH4 methyltransferases. *Mol. Cell. Biol.*, **25**, 10507–10515.
22. Naumann,K., Fischer,A., Hofmann,I., Krauss,V., Phalke,S., Irmler,K., Hause,G., Aurich,A., Dorn,R., Jenuwein,T. *et al.* (2005) Pivotal role of AtSUVH2 in heterochromatic histone methylation and gene silencing in *Arabidopsis*. *EMBO J.*, **24**, 1418–1429.
23. Murray,M. and Thompson,F. (1980) Rapid isolation of high molecular weight plant DNA. *Nucleic Acids Res.*, **8**, 4321–4325.
24. Yanisch-Perron,C., Vieira,J. and Messing,J. (1985) Improved M13 phage cloning vectors and host strains: nucleotide sequences of the M13mp18 and pUC19 vectors. *Gene*, **33**, 103–119.

25. Gendrel,A., Lippman,Z., Martienssen,R. and Colot,V. (2005) Profiling histone modification patterns in plants using genomic tiling microarrays. *Nat. Methods*, **2**, 213–218.

26. Lippman,Z., Gendrel,A., Colot,V. and Martienssen,R. (2005) Profiling DNA methylation patterns using genomic tiling microarrays. *Nat. Methods*, **2**, 219–224.

27. Richards,E. and Ausubel,F. (1988) Isolation of a higher eukaryotic telomere from *Arabidopsis thaliana*. *Cell*, **53**, 127–136.

28. Richards,E., Goodman,H. and Ausubel,F. (1991) The centromere region of *Arabidopsis thaliana* chromosome 1 contains telomere-similar sequences. *Nucleic Acids Res.*, **19**, 3351–3357.

29. Richards,E., Chao,S., Vongs,A. and Yang,J. (1992) Characterization of *Arabidopsis thaliana* telomeres isolated in yeast. *Nucleic Acids Res.*, **20**, 4039–4046.

30. Regad,F., Lebas,M. and Lescure,B. (1994) ITSs within the *Arabidopsis thaliana* genome. *J. Mol. Biol.*, **239**, 163–169.

31. Uchida,W., Matsunaga,S., Sugiyama,R. and Kawano,S. (2002) Interstitial telomere-like repeats in the *Arabidopsis thaliana* genome. *Genes Genet. Syst.*, **77**, 63–67.

32. Shakirov,E. and Shippen,D. (2004) Length regulation and dynamics of individual telomere tracts in wild-type *Arabidopsis*. *Plant Cell*, **16**, 1959–1967.

33. Fitzgerald,M., Riha,K., Gao,F., Ren,S., McKnight,T. and Shippen,D. (1999) Disruption of the telomerase catalytic subunit gene from *Arabidopsis* inactivates telomerase and leads to a slow loss of telomeric DNA. *Proc. Natl Acad. Sci. USA*, **96**, 14813–14818.

34. Gallego,M. and White,C. (2001) RAD50 function is essential for telomere maintenance in *Arabidopsis*. *Proc. Natl Acad. Sci. USA*, **98**, 1711–1716.

35. Gámez-Arjona,F., López-López,C., Vaquero-Sedas,M. and Vega-Palas,M. (2010) On the organization of the nucleosomes associated with telomeric sequences. *Biochim. Biophys. Acta*, **1803**, 1058–1061.

36. Vannier,J., Depeiges,A., White,C. and Gallego,M. (2009) ERCC1/ XPF protects short telomeres from homologous recombination in *Arabidopsis thaliana*. *PLoS Genet.*, **5**, e1000380.

37. Riha,K., Watson,J., Parkey,J. and Shippen,D. (2002) Telomere length deregulation and enhanced sensitivity to genotoxic stress in *Arabidopsis* mutants deficient in Ku70. *EMBO J.*, **21**, 2819–2826.

38. Bernatavichute,Y., Zhang,X., Cokus,S., Pellegrini,M. and Jacobsen,S. (2008) Genome-wide association of histone H3 lysine nine methylation with CHG DNA methylation in *Arabidopsis thaliana*. *PLoS One*, **3**, e3135.

39. Zhang,X., Yazaki,J., Sundaresan,A., Cokus,S., Chan,S., Chen,H., Henderson,I., Shinn,P., Pellegrini,M., Jacobsen,S. *et al.* (2006) Genome-wide high-resolution mapping and functional analysis of DNA methylation in *Arabidopsis*. *Cell*, **126**, 1189–1201.

40. Zhang,X., Bernatavichute,Y., Cokus,S., Pellegrini,M. and Jacobsen,S. (2009) Genome-wide analysis of mono-, di- and trimethylation of histone H3 lysine 4 in *Arabidopsis thaliana*. *Genome Biol.*, **10**, R62.

41. Krauss,V. (2008) Glimpses of evolution: heterochromatic histone H3K9 methyltransferases left its marks behind. *Genetica*, **133**, 93–106.

42. Millar,C. and Grunstein,M. (2006) Genome-wide patterns of histone modifications in yeast. *Nat. Rev. Mol. Cell. Biol.*, **7**, 657–666.

43. Vrbsky,J., Akimcheva,S., Watson,J., Turner,T., Daxinger,L., Vyskot,B., Aufsatz,W. and Riha,K. (2010) siRNA-mediated methylation of *Arabidopsis* telomeres. *PLoS Genet.*, **6**, e1000986.

44. Gendrel,A. and Colot,V. (2005) *Arabidopsis* epigenetics: when RNA meets chromatin. *Curr. Opin. Plant Biol.*, **8**, 142–147.

45. Henderson,I. and Jacobsen,S. (2007) Epigenetic inheritance in plants. *Nature*, **447**, 418–424.

46. Vaughn,M. and Martienssen,R. (2005) It's a small RNA world, after all. *Science*, **309**, 1525–1526.

47. Gustafson,A., Allen,E., Givan,S., Smith,D., Carrington,J. and Kasschau,K. (2005) ASRP: the *Arabidopsis* small RNA project database. *Nucleic Acids Res.*, **33**, D637–D640.

48. Watson,J. and Riha,K. (2010) Comparative biology of telomeres: where plants stand. *FEBS Lett.*, **584**, 3752–3759.

49. Lin,K. and Yan,J. (2008) Endings in the middle: current knowledge of interstitial telomeric sequences. *Mutation Res.*, **658**, 95–110.

50. Peng,J. and Karpen,G. (2008) Epigenetic regulation of heterochromatic DNA stability. *Curr. Opin. Genet. Dev.*, **18**, 204–211.